European Conference on Computational Fluid Dynamics
ECCOMAS CFD 2006
P. Wesseling, E. Oñate and J. Périaux (Eds)

GODUNOV SCHEMES FOR COMPRESSIBLE MULTIPHASE FLOWS

C. E. Castro* and E. F. Toro*

*University of Trento, Laboratory of Applied Mathematics, Faculty of Engineering
Mesiano 77, 38050 Trento, Italy
e-mail: castroc@ing.unitn.it, toro@ing.unitn.it
web page:http://www.ing.unitn.it/∼castroc, http://www.ing.unitn.it/toro

Key words: Godunov schemes, Multiphase flows, Riemann solvers

Abstract. *Compressible multiphase models have been studied for a long time inspired on different applications in diverse engineering areas. Solutions for these equations are not simple and researcher have spent much time trying to bring answers. The possibility to properly solve these equations and perform real simulations represent a very ambitious goal. Today new numerical techniques show a promising path to reach the goal.*

We are concerned with the construction of Godunov-type schemes for compressible multiphase flows. In particular we study finite volume methods for the Baer-Nunziato equations,[1] a system of seven equations for the 1D case.

First we assess the stratified approach reported in,[2] whereby the two-phase Riemann problem is reduced to a set of simpler ones in which the initial states are single phases.

Then we propose the extension of the EVILIN[3] approach to solve approximately the complete two phase Riemann problem. Numerical results for test problems with exact solutions[4] are presented.

1 INTRODUCTION

For nearly 30 years multiphase models have been widely studied and a number of models have been proposed, see for example Baer-Nunziato[1] for deflagration to detonation transition and Saurel-Abgrall[5] for two compressible fluids. See also Romenski,[8] Stewart and Wendroff,[9] Drew,[10] Ishii[11] or Gidaspow[12] amongst others. It is known today that the fact of having two pressure models preserves hyperbolicity. Considering numerical methods for hyperbolic equations the experience is vast for simple problems, now this experience is coming into multiphase models and a major effort has been put into it, for example the work of Andrianov and Warnecke with their inverse problem,[7] Chang and Liou,[16] Abgrall[13] or Schwendeman et al.[4] where an iterative two step Riemann solver is used, amongst others.

The work[4] is very interesting where they manage to solve the complete Riemann problem iteratively, in a similar way as the Riemann solver presented in Castro and Toro[6]

for the Saurel-Abgrall isentropic model. Here the key point is to find proper jump relations across the solid contact, making use of an auxiliary variable and then solving the decoupled system for the solid and gas phase. As Schwendeman et al. say in the article, this procedure is expensive in computational time and a less expensive procedure is still needed.

In this article we deal with the problem of approximating solutions of compressible multiphase flow using finite volume numerical methods of the Godunov type. A major problem is the calculation of the numerical fluxes, which in the Godunov approach come from the solution of the Riemann problem.

Two approaches are used to solve the Riemann problem: one applies the EVILIN Riemann solver and the other uses a stratification hypothesis[2] prior to the application of the EVILIN[3] or the exact Riemann solver.[14] Because the interaction between the two phases represents a major difficult numerically, which results in a contact wave, complete Riemann solvers are needed. Numerical results for typical test problems are presented, including convergence rate tests.

The paper is organized as follow: in section 2 the Baer-Nunziato multiphase model is written; in section 3 the numerical method is developed; in section 4 test problems are presented and finally in section 5 conclusions are drawn.

2 THE BAER-NUNZIATO MULTIPHASE MODEL

The multiphase model proposed by Baer-Nunziato[1] represents the interaction between two compressible fluids considering non-equilibrium pressure. Originally presented as a deflagration to detonation transition model (DDT) was analized by Embid et al.[15] The two compressible fluids are denoted by suffixes $k = 1,\ 2$. The interphase velocity and pressure are respectively denoted by u_1, p_2. Due to the presence of interphase terms the system cannot be cast in conservative form. Neglecting exchange terms such as chemical reactions and drag forces, the homogeneous one dimensional model is written in (1), using the regular notation where ρ_k denotes density, u_k is particle velocity, p_k is pressure, $E_k = \rho_k(\frac{1}{2}u_k^2 + e_k)$ is total energy, e_k is specific energy and α_k is the void fraction, assuming $\sum \alpha_k = 1$.

$$
\left.
\begin{array}{l}
\frac{\partial}{\partial t}(\alpha_1\rho_1) + \frac{\partial}{\partial x}(\alpha_1\rho_1 u_1) = 0 \\
\frac{\partial}{\partial t}(\alpha_1\rho_1 u_1) + \frac{\partial}{\partial x}(\alpha_1[\rho_1 u_1^2 + p_1]) - p_2\frac{\partial}{\partial x}(\alpha_1) = 0 \\
\frac{\partial}{\partial t}(\alpha_1 E_1) + \frac{\partial}{\partial x}(\alpha_1 u_1[E_1 + p_1]) - p_2 u_1\frac{\partial}{\partial x}(\alpha_1) = 0 \\
\frac{\partial}{\partial t}(\alpha_2\rho_2) + \frac{\partial}{\partial x}(\alpha_2\rho_2 u_2) = 0 \\
\frac{\partial}{\partial t}(\alpha_2\rho_2 u_2) + \frac{\partial}{\partial x}(\alpha_2[\rho_2 u_2^2 + p_2]) + p_2\frac{\partial}{\partial x}(\alpha_1) = 0 \\
\frac{\partial}{\partial t}(\alpha_2 E_2) + \frac{\partial}{\partial x}(\alpha_2 u_2[E_2 + p_2]) + p_2 u_1\frac{\partial}{\partial x}(\alpha_1) = 0 \\
\frac{\partial}{\partial t}(\alpha_1) + u_1\frac{\partial}{\partial x}(\alpha_1) = 0
\end{array}
\right\} \qquad (1)
$$

The first three equations in (1) represent the space and time evolution of fluid 1, as the classical gas dynamic Euler system, plus the inclusion of the interaction terms between both phases. An analogous description applies for the fourth to sixth equations for fluid 2. The seventh equation is a closing relation that represents the advection of the interface between fluids. For both fluids the stiffened equation of state (EOS) is used giving properly values for γ_k and p_k^o. The specific energy e_k and sound speed a_k are,

$$e_k = \frac{p_k + \gamma_k p_k^o}{\rho_k(\gamma_k - 1)}, \qquad a_k^2 = (\gamma_k - 1)(\frac{p_k}{\rho_k} + e_k) \tag{2}$$

System (1) can be written in vectorial notation as follows,

$$\partial_t \mathbf{Q} + \partial_x \mathbf{F}(\mathbf{Q}) + \mathbf{A}(\mathbf{Q})\ \partial_x \mathbf{W}(\mathbf{Q}) = \mathbf{S}(\mathbf{Q}), \tag{3}$$

where vector $\mathbf{Q}$ is the conservative unknown vector, $\mathbf{F}(\mathbf{Q})$ is a flux, $\mathbf{A}(\mathbf{Q})$ is a coefficient matrix with variable entries. Equation (3) represents a general hyperbolic system with conservative and non-conservative terms and their choice is somewhat arbitrary. In our experience the following represents the most desirable combination for system (1).

$$\mathbf{Q} = \begin{bmatrix} \alpha_1\rho_1 \\ \alpha_1\rho_1 u_1 \\ \alpha_1 E_1 \\ \alpha_2\rho_2 \\ \alpha_2\rho_2 u_2 \\ \alpha_2 E_2 \\ \alpha_1 \end{bmatrix} \qquad \mathbf{F}(\mathbf{Q}) = \begin{bmatrix} \alpha_1\rho_1 u_1 \\ \alpha_1[\rho_1 u_1^2 + p_1] \\ \alpha_1 u_1[E_1 + p_1] \\ \alpha_2\rho_2 u_2 \\ \alpha_2[\rho_2 u_2^2 + p_2] \\ \alpha_2 u_2[E_2 + p_2] \\ 0 \end{bmatrix} \tag{4}$$

$$\mathbf{A}(\mathbf{Q}) = \begin{bmatrix} 0 & 0 & 0 & 0 & 0 & 0 & 0 \\ 0 & 0 & 0 & 0 & 0 & 0 & -p_2 \\ 0 & 0 & 0 & 0 & 0 & 0 & -p_2 u_1 \\ 0 & 0 & 0 & 0 & 0 & 0 & 0 \\ 0 & 0 & 0 & 0 & 0 & 0 & p_2 \\ 0 & 0 & 0 & 0 & 0 & 0 & p_2 u_1 \\ 0 & 0 & 0 & 0 & 0 & 0 & u_1 \end{bmatrix} \qquad \mathbf{W}(\mathbf{Q}) = \begin{bmatrix} \rho_1 \\ u_1 \\ p_1 \\ \rho_2 \\ u_2 \\ p_2 \\ \alpha_1 \end{bmatrix} \tag{5}$$

An alternative formulation for system (1) is the fully non-conservative one where the unknowns are the physical variables. This formulation will allow us to extract very useful information from the eigenstructure of the system which in quasi-linear form reads.

$$\partial_t \mathbf{W} + \mathbf{B}(\mathbf{W})\partial_x \mathbf{W} = 0\ , \tag{6}$$

where $\mathbf{W}$ is the vector of physical variables and $\mathbf{B}(\mathbf{W})$ is the Jacobian matrix.

$$\mathbf{W} = \begin{bmatrix} \rho_1 \\ u_1 \\ p_1 \\ \rho_2 \\ u_2 \\ p_2 \\ \alpha_1 \end{bmatrix} \quad \mathbf{B}(\mathbf{W}) = \begin{bmatrix} u_1 & \rho_1 & 0 & 0 & 0 & 0 & 0 \\ 0 & u_1 & \frac{1}{\rho_1} & 0 & 0 & 0 & \frac{p_1 - p_2}{\alpha_1 \rho_1} \\ 0 & a_1^2 \rho_1 & u_1 & 0 & 0 & 0 & 0 \\ 0 & 0 & 0 & u_2 & \rho_2 & 0 & \frac{\rho_2 (u_1 - u_2)}{\alpha_2} \\ 0 & 0 & 0 & 0 & u_2 & \frac{1}{\rho_2} & 0 \\ 0 & 0 & 0 & 0 & a_2^2 \rho_2 & u_2 & \frac{a_2^2 \rho_2 (u_1 - u_2)}{\alpha_2} \\ 0 & 0 & 0 & 0 & 0 & 0 & u_1 \end{bmatrix} \tag{7}$$

The (real) eigenvalues are

$$\lambda_1 = u_1 - a_1,\ \lambda_2 = u_2 - a_2,\ \lambda_3 = u_2,\ \lambda_4 = \lambda_5 = u_1,\ \lambda_6 = u_2 + a_2,\ \lambda_7 = u_1 + a_1 \tag{8}$$

with corresponding right eigenvectors

$$\mathbf{R}^{(1)} = \begin{bmatrix} -\rho_1/a_1 \\ 1 \\ -\rho_1 a_1 \\ 0 \\ 0 \\ 0 \\ 0 \end{bmatrix},\ \mathbf{R}^{(2)} = \begin{bmatrix} 0 \\ 0 \\ 0 \\ -\rho_2/a_2 \\ 1 \\ -\rho_2 a_2 \\ 0 \end{bmatrix},\ \mathbf{R}^{(3)} = \begin{bmatrix} 0 \\ 0 \\ 0 \\ 1 \\ 0 \\ 0 \\ 0 \end{bmatrix},\ \mathbf{R}^{(4)} = \begin{bmatrix} 1 \\ 0 \\ 0 \\ 0 \\ 0 \\ 0 \\ 0 \end{bmatrix}, \tag{9}$$

$$\mathbf{R}^{(5)} = \begin{bmatrix} 0 \\ 0 \\ \frac{\alpha_2 (p_2 - p_1)\left((u_1 - u_2)^2 - a_2^2\right)}{\alpha_1 \rho_2} \\ (u_1 - u_2)^2 \\ \frac{-a_2^2 (u_1 - u_2)}{\rho_2} \\ a_2^2 (u_1 - u_2)^2 \\ \frac{\alpha_2 \left((u_1 - u_2)^2 - a_2^2\right)}{\rho_2} \end{bmatrix},\ \mathbf{R}^{(6)} = \begin{bmatrix} 0 \\ 0 \\ 0 \\ \rho_2/a_2 \\ 1 \\ \rho_2 a_2 \\ 0 \end{bmatrix},\ \mathbf{R}^{(7)} = \begin{bmatrix} \rho_1/a_1 \\ 1 \\ \rho_1 a_1 \\ 0 \\ 0 \\ 0 \\ 0 \end{bmatrix}, \tag{10}$$

From (8) we see that all eigenvalues of $\mathbf{B}(\mathbf{W})$ are real; however they are not distinct and therefore this system is not strictly hyperbolic. Possible singular points are: (a) $u_1 = u_2$, (b) $u_1 = u_2 \pm a_2$, (c) $u_1 \pm a_1 = u_2$, and (d) $u_1 \pm a_1 = u_2 \pm a_2$. Condition (b), called sonic condition or *chocked flow condition*, represents a real problem in which case the eigenvectors do not form a complete set of linear independent vector.

Characteristic fields associated with λ_1, λ_2, λ_6 and λ_7 are *genuinely non-linear fields* consequently shock or rarefaction waves are produced. Waves associated to λ_3, λ_4 and

λ_5 are *linearly degenerated fields* therefore contact waves are produced, more over, λ_3 is associated to fluid 2, λ_4 is associated to fluid 1 and λ_5 connect both fluids and collide with λ_4. For details see the work of Embid and Baer.[15]

In the following, two numerical methods are constructed for solving this system. The first one solve the Riemann problem considering the hole system applying the EVILIN[3] approach while the second one assume a stratification hypothesis[2] and simpler problems are solved before constructing the solution of the full system.

3 NUMERICAL METHODS

Integrating equation (3) over the control volume $V_i = [x_{i-1/2}, x_{i+1/2}] \times [t^n, t^{n+1}]$ in $x-t$ space with $x = i\Delta x$, $t = n\Delta t$ and assuming a local linearization of $\mathbf{A}(\mathbf{Q})$ we have

$$\mathbf{Q}_i^{n+1} = \mathbf{Q}_i^n - \frac{\Delta t}{\Delta x}\left[\mathbf{F}_{i+\frac{1}{2}} - \mathbf{F}_{i-\frac{1}{2}}\right] - \frac{\Delta t}{\Delta x}\mathbf{A}_i\left[\mathbf{W}_{i+\frac{1}{2}} - \mathbf{W}_{i-\frac{1}{2}}\right] + \Delta t \mathbf{S}_i \tag{11}$$

$$\begin{aligned}
\mathbf{Q}_i^n &\approx \tfrac{1}{\Delta x}\int_{x_{i-\frac{1}{2}}}^{x_{i+\frac{1}{2}}} \mathbf{Q}(\chi, t^n)\, d\chi \\
\mathbf{F}_{i+\frac{1}{2}} &\approx \tfrac{1}{\Delta t}\int_{t^n}^{t^{n+1}} \mathbf{F}(\mathbf{Q}(x_{i+\frac{1}{2}}, \tau))\, d\tau \\
\mathbf{W}_{i+\frac{1}{2}} &\approx \tfrac{1}{\Delta t}\int_{t^n}^{t^{n+1}} \mathbf{W}(\mathbf{Q}(x_{i+\frac{1}{2}}, \tau))\, d\tau \\
\mathbf{A}_i &= \mathbf{A}\left(\tfrac{1}{2}(\mathbf{W}_{i+\frac{1}{2}} + \mathbf{W}_{i-\frac{1}{2}})\right) \\
\mathbf{S}_i &\approx \tfrac{1}{\Delta x \Delta t}\int_{t^n}^{t^{n+1}}\int_{x_{i-\frac{1}{2}}}^{x_{i+\frac{1}{2}}} \mathbf{S}(\mathbf{Q}(\chi, \tau))\, d\chi\, d\tau
\end{aligned} \tag{12}$$

In (12) $\mathbf{Q}_i^n$ is a spatial integral average within volume i of length Δx at time level n, $\mathbf{F}_{i+\frac{1}{2}}$ is the numerical flux at the interface $x = x_{i+\frac{1}{2}}$ integrated in time from t^n to t^{n+1} while $\mathbf{W}_{i+\frac{1}{2}}$ is a time integral average of the state at the same interface; the coefficient matrix $\mathbf{A}_i$ is an average within the cell i and the source term $\mathbf{S}_i$ is an approximation to a space-time integral over the control volume V_i; Δt is the time step computed from a stability condition in the range $0 < C_{cfl} \leq 1$, where C_{cfl} is the usual Courant number coefficient. Scheme (11) is an explicit one step method for updating cell average. The scheme is defined once an intercell quantities and numerical sources are known. A key quantity is $\mathbf{Q}_{i+\frac{1}{2}}$. For a first-order method this is obtained by the classical Riemann problem.

$$\left.\begin{array}{rcl} \partial_t \mathbf{Q} + \partial_x \mathbf{F}(\mathbf{Q}) + \mathbf{A}(\mathbf{Q})\, \partial_x \mathbf{W}(\mathbf{Q}) & = & \mathbf{S}(\mathbf{Q}), \\ \mathbf{Q}(x,0) & = & \left\{ \begin{array}{llll} \mathbf{Q}_L = \mathbf{Q}_i^n & if & x < x_{i+\frac{1}{2}} \\ \mathbf{Q}_R = \mathbf{Q}_{i+1}^n & if & x > x_{i+\frac{1}{2}} \end{array} \right. \end{array}\right\} \tag{13}$$

Solving the Riemann problem (13) with pice-wise constant data have been a goal for

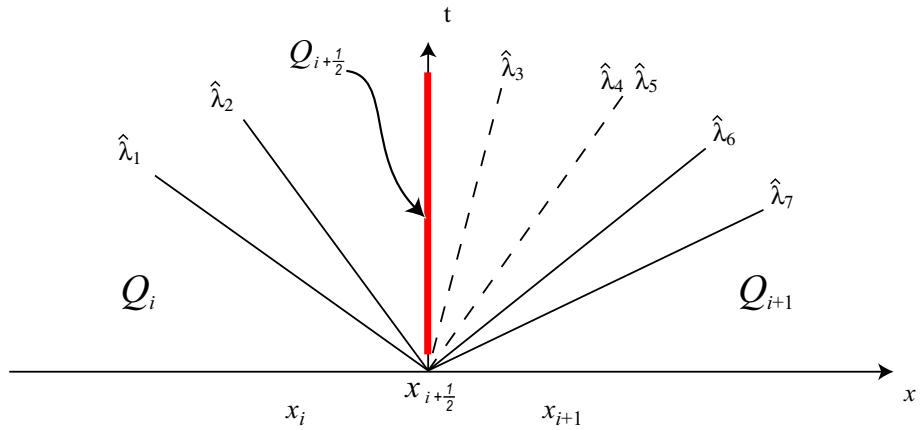

Figure 1: Riemann problem for the full system with initial data $\mathbf{Q}_i$ and $\mathbf{Q}_{i+1}$. The fan is opened with seven waves and the intercell state $\mathbf{Q}_{i+\frac{1}{2}}$ is on the t-axes

many years. There are two ways of going about to calculate interface quantities and thus to determine a numerical schemes. These are the subjects of the following two sections.

3.1 Stratified formulation

The stratified formulation of our interest was reported in[2] where the two-phase Riemann problem is reduced to a set of simpler ones in for single phases. These simpler problems obey the single phase gas dynamic Euler system for which more choices to solve the Riemann problem are available. Here we will couple this formulation with the exact and EVILIN Riemann solvers.

In general multifluid models are constructed from averaging techniques[11] where the ratio of the volume occupied by each fluid is known but not the spatial distribution. Applying the stratified hypothesis this spatial distribution is constructed based on the void fraction α_k producing a very interesting configuration. In figure 2 this is graphically represented, where two adjacent cells contain a mixture of two phases and after the hypothesis a clear stratified representation is shown where three interfaces are clearly visibly. Four interactions are possible depending the void fraction in each cell. These interaction account for: fluid 1 - fluid 1, fluid 1 - fluid 2, fluid 2 - fluid 1 and fluid 2 - fluid 2. Each interaction has a weight ω_l with $l = 1, 2, 3, 4$ defined as follow

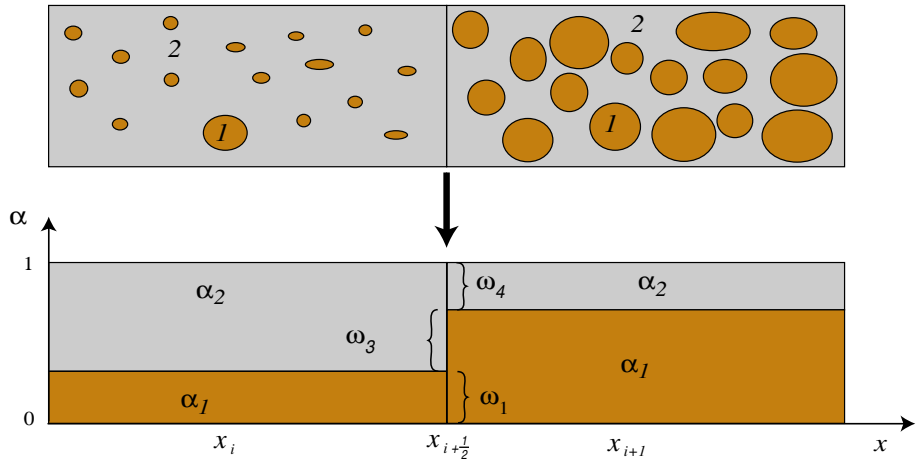

Figure 2: Stratified approach: The upper figure shows two adjacent cells with two fluid mixtures. The bottom figure shows the representation of the data after applying the stratification hypothesis.

$$\begin{array}{rclrcl} \omega_1 &=& min\{\alpha_{1i}, \alpha_{1i+1}\} & \omega_4 &=& min\{\alpha_{2i}, \alpha_{2i+1}\} \\ \omega_2 &=& max\{0, \alpha_{1i} - \alpha_{1i+1}\} & \omega_3 &=& max\{0, \alpha_{2i} - \alpha_{2i+1}\} \end{array}, \tag{14}$$

with the conditions $\omega_2 \cdot \omega_3 = 0$ and $\omega_1 + \omega_2 + \omega_3 + \omega_4 = 1$. With these weights it is possible to compute the intercell state $\mathbf{Q}_{i+\frac{1}{2}} = \omega_1 \mathbf{Q}^{(1)}_{i+\frac{1}{2}} + \omega_2 \mathbf{Q}^{(2)}_{i+\frac{1}{2}} + \omega_3 \mathbf{Q}^{(3)}_{i+\frac{1}{2}} + \omega_4 \mathbf{Q}^{(4)}_{i+\frac{1}{2}}$ where $\mathbf{Q}^{(l)}_{i+\frac{1}{2}}$ is the solution of the Riemann problem for a single phase Euler system.

$$\left.\begin{array}{rcl} \partial_t \mathbf{Q} + \partial_x \mathbf{F}(\mathbf{Q}) &=& 0 \\ \mathbf{Q}(\mathbf{x}, \mathbf{0}) &=& \left\{ \begin{array}{rcll} \mathbf{Q}_L &=& Q_{k,i} & if \;\; x < x_{i+\frac{1}{2}} \\ \mathbf{Q}_R &=& Q_{k,i+1} & if \;\; x > x_{i+\frac{1}{2}} \end{array} \right. \end{array}\right\} \tag{15}$$

The initial data $Q_{k,i}$ and $Q_{k,i+1}$ with $k = 1, 2$ are computed for cell i as

$$\mathbf{Q}_i = \left[\begin{array}{c} \alpha_1\rho_1 \\ \alpha_1\rho_1 u_1 \\ \alpha_1 E_1 \\ \alpha_2\rho_2 \\ \alpha_2\rho_2 u_2 \\ \alpha_2 E_2 \\ \alpha_1 \end{array} \right]_i \Rightarrow \begin{array}{l} \mathbf{Q}_{1,i} = \left[\begin{array}{c} \rho_1 \\ \rho_1 u_1 \\ E_1 \end{array} \right]_i \\ \\ \mathbf{Q}_{2,i} = \left[\begin{array}{c} \rho_2 \\ \rho_2 u_2 \\ E_2 \end{array} \right]_i \end{array} \tag{16}$$

The Riemann problems 15 have a well known wave structure. The velocity u^* between each pair of non-linear waves, (the velocity of the contact wave) plays a very important role. We define the pair $\{k_L, k_R\}$ with $k_L = 1, 2$ and $k_R = 1, 2$ for all combinations between fluid 1 or 2 into cell i(L) or $i + 1$(R). Following Table 1 the solution of the Riemann problem is correctly assigned to $\mathbf{Q}^{(l)}_{i+\frac{1}{2}}$.

k_L	k_R	l
1	1	1
2	2	4
1	2	$2 \ if \ u^* > 0$
1	2	$3 \ if \ u^* < 0$
2	1	$2 \ if \ u^* < 0$
2	1	$3 \ if \ u^* > 0$

Table 1: Correct assignment for intercell vectors $\mathbf{Q}^{(l)}_{i+\frac{1}{2}}$

3.2 EVILIN Riemann solver for a non conservative formulation

In this section we present the EVILIN Riemann solver for the Baer-Nunziato system. EVILIN approach was presented by Toro[3] and the idea is to evolve the initial data by a simple scheme and solve a linear Riemann problem with evolved data as initial condition. EVILIN follows the framework of the MUSTA[19] Riemann solver, but includes upwind information. In figure 3 the initial data $\mathbf{Q}_0 = \mathbf{Q}_i$ and $\mathbf{Q}_1 = \mathbf{Q}_{i+1}$ is evolved to $\bar{\mathbf{Q}}_L$ and $\bar{\mathbf{Q}}_R$ using the non conservative step of equations (17-18).

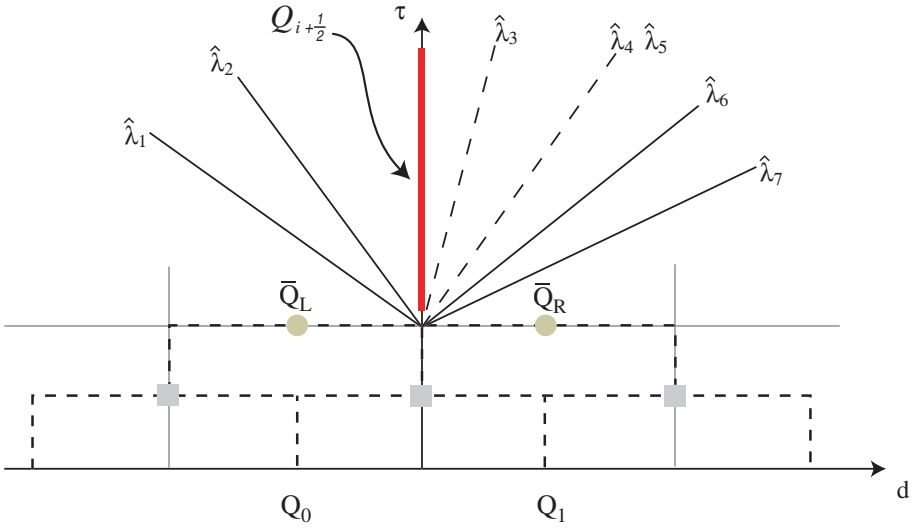

Figure 3: Evilin Riemann solver for non conservative formulation. $\mathbf{Q}_0$ and $\mathbf{Q}_1$ is the initial data evolved to $\bar{\mathbf{Q}}_L$ and $\bar{\mathbf{Q}}_R$ which is solved with a linear solver in order to obtain $\mathbf{Q}_{i+\frac{1}{2}}$. All performed in local space $\chi - \tau$

$$
\begin{aligned}
\mathbf{Q}_L^{\frac{1}{2}} &= \mathbf{Q}_0 \\
\mathbf{Q}_C^{\frac{1}{2}} &= \tfrac{1}{2}(\mathbf{Q}_0 + \mathbf{Q}_1) - \tfrac{1}{2}\tfrac{\Delta\tau}{\Delta d}\left[\mathbf{F}(\mathbf{Q}_1) - \mathbf{F}(\mathbf{Q}_0)\right] - \tfrac{1}{2}\tfrac{\Delta\tau}{\Delta d}\tilde{\mathbf{A}}_C^{\frac{1}{2}}\left[\mathbf{W}(\mathbf{Q}_1) - \mathbf{W}(\mathbf{Q}_0)\right] \\
\tilde{\mathbf{A}}_C^{\frac{1}{2}} &= \mathbf{A}\left(\tfrac{1}{2}(\mathbf{Q}_0 + \mathbf{Q}_1)\right) \\
\mathbf{Q}_R^{\frac{1}{2}} &= \mathbf{Q}_1
\end{aligned}
\tag{17}
$$

$$
\begin{aligned}
\bar{\mathbf{Q}}_L &= \tfrac{1}{2}(\mathbf{Q}_L^{\frac{1}{2}} + \mathbf{Q}_C^{\frac{1}{2}}) - \tfrac{1}{2}\tfrac{\Delta\tau}{\Delta d}\left[\mathbf{F}(\mathbf{Q}_C^{\frac{1}{2}}) - \mathbf{F}(\mathbf{Q}_L^{\frac{1}{2}})\right] - \tfrac{1}{2}\tfrac{\Delta\tau}{\Delta d}\tilde{\mathbf{A}}_L\left[\mathbf{W}(\mathbf{Q}_C^{\frac{1}{2}}) - \mathbf{W}(\mathbf{Q}_L^{\frac{1}{2}})\right] \\
\bar{\mathbf{Q}}_R &= \tfrac{1}{2}(\mathbf{Q}_C^{\frac{1}{2}} + \mathbf{Q}_R^{\frac{1}{2}}) - \tfrac{1}{2}\tfrac{\Delta\tau}{\Delta d}\left[\mathbf{F}(\mathbf{Q}_R^{\frac{1}{2}}) - \mathbf{F}(\mathbf{Q}_C^{\frac{1}{2}})\right] - \tfrac{1}{2}\tfrac{\Delta\tau}{\Delta d}\tilde{\mathbf{A}}_R\left[\mathbf{W}(\mathbf{Q}_R^{\frac{1}{2}}) - \mathbf{W}(\mathbf{Q}_C^{\frac{1}{2}})\right] \\
\tilde{\mathbf{A}}_L &= \mathbf{A}\left(\tfrac{1}{2}(\mathbf{Q}_L^{\frac{1}{2}} + \mathbf{Q}_C^{\frac{1}{2}})\right) \\
\tilde{\mathbf{A}}_R &= \mathbf{A}\left(\tfrac{1}{2}(\mathbf{Q}_C^{\frac{1}{2}} + \mathbf{Q}_R^{\frac{1}{2}})\right)
\end{aligned}
\tag{18}
$$

Once the initial data have been evolved to $\bar{\mathbf{Q}}_L$ and $\bar{\mathbf{Q}}_R$, a linear Riemann solver is used in order to find the intercell state $\mathbf{Q}_{i+1/2}$ solving the initial value problem (19).

$$
\left.
\begin{aligned}
\partial_t \mathbf{W} + \hat{\mathbf{B}}\partial_x \mathbf{W} &= 0, \\
\mathbf{W}(x,0) &= \begin{cases} \mathbf{W}_L \equiv \mathbf{W}(\bar{\mathbf{Q}}_L) & if \quad x < 0 \\ \mathbf{W}_R \equiv \mathbf{W}(\bar{\mathbf{Q}}_R) & if \quad x > 0 \end{cases}
\end{aligned}
\right\}
\tag{19}
$$

$\mathbf{Q}_{i+1/2}$ is used in (11) for updating cell averages.

3.3 The MUSCL_Hancock method

A second order scheme[17] can be constructed using the MUSCL_Hancock approach. Data reconstruction is performed using piece wise linear functions and boundary extrapolated values are evolved by half a time step and then used as initial data for a piece-wise constant data Riemann problem. Non oscillatory properties come from TVD slope limiters applied to the data reconstruction step. See[18] for more details. The piece wise linear reconstruction has boundary extrapolated values

$$
\mathbf{W}_i^L = \mathbf{W}_i^n - \frac{1}{2}\Delta_i \ , \qquad \mathbf{W}_i^R = \mathbf{W}_i^n + \frac{1}{2}\Delta_i \ ,
\tag{20}
$$

where

$$
\boldsymbol{\Delta}_i = \frac{1}{2}(1+\omega)\boldsymbol{\Delta}_{i-\frac{1}{2}} + \frac{1}{2}(1-\omega)\boldsymbol{\Delta}_{i+\frac{1}{2}} \ ,
$$

$$
\boldsymbol{\Delta}_{i-\frac{1}{2}} = \mathbf{W}_i - \mathbf{W}_{i-1} \ , \ \ \boldsymbol{\Delta}_{i+\frac{1}{2}} = \mathbf{W}_{i+1} - \mathbf{W}_i \ ,
$$

with $\omega \, \epsilon \, [-1, 1]$. The boundary extrapolated values (20) are evolved thus

$$
\overline{\mathbf{W}}_i^L = \mathbf{W}_i^L + \frac{1}{2}\frac{\Delta t}{\Delta x}\widetilde{\mathbf{B}}_i\left[\mathbf{W}_i^L - \mathbf{W}_i^R\right] \ ,
\tag{21}
$$

$$
\overline{\mathbf{W}}_i^R = \mathbf{W}_i^R + \frac{1}{2}\frac{\Delta t}{\Delta x}\widetilde{\mathbf{B}}_i\left[\mathbf{W}_i^L - \mathbf{W}_i^R\right] \ ,
\tag{22}
$$

leading to the expressions

$$
\overline{\mathbf{W}}_i^L = \mathbf{W}_i^n - \frac{1}{2}\left[\mathrm{I} + \frac{\Delta t}{\Delta x}\widetilde{\mathbf{B}}_i\right]\Delta_i \ , \ \ \overline{\mathbf{W}}_i^R = \mathbf{W}_i^n + \frac{1}{2}\left[\mathrm{I} - \frac{\Delta t}{\Delta x}\widetilde{\mathbf{B}}_i\right]\Delta_i \ ,
\tag{23}
$$

where the coefficient matrix is taken as $\widetilde{\mathbf{B}}_i = \mathbf{B}(\mathbf{W}_i^n)$. The extrapolated values will be used in any of the method presented in section 3.1 or 3.2 as initial conditions.

4 TEST PROBLEMS

In this section we present two test problems to assess the numerical solutions. The first test is a shock tube problem for liquid and gas, while the second one is a convergence test. For each test three numerical solutions are shown, EVILIN, StraEv and StraEx. EVILIN comes from applying the EVILIN Riemann solver to the full seven equation system. StraEv comes from applying the stratification hypothesis plus EVILIN Riemann solver for the interaction between identical fluids and the exact Riemann solver for different fluids. Finally, StarEx consist of the stratification hypothesis plus the exact Riemann solver for all interactions. For test 1, first and second order numerical solutions are presented with two meshes, 100 and 800 cells. For test 2 a smooth initial condition is set and evolved until $t = 0.1$.

4.1 Test 1: Shock tube problem for liquid and gas

This test problem generates the interaction between one liquid and one gas with the following constants for the equation of state: $\gamma_1 = 4.4$, $p_1^o = 6.0 \times 10^8$, $\gamma_2 = 1.4$ and $p_2^o = 0.0$. The initial discontinuity is at $x = 0.5$, the CFL coefficient is $C_{cfl} = 0.5$ and the output time is $t = 0.25 \times 10^{-3}$ s. The wave structure of the solution is shown in figure 4. Rarefaction waves travelling to the left are present in both fluids and shock waves travel to the right, also in both fluids. All three contact waves travel slowly to the right and are indistinguishable from each other. Initial conditions are given in table 2.

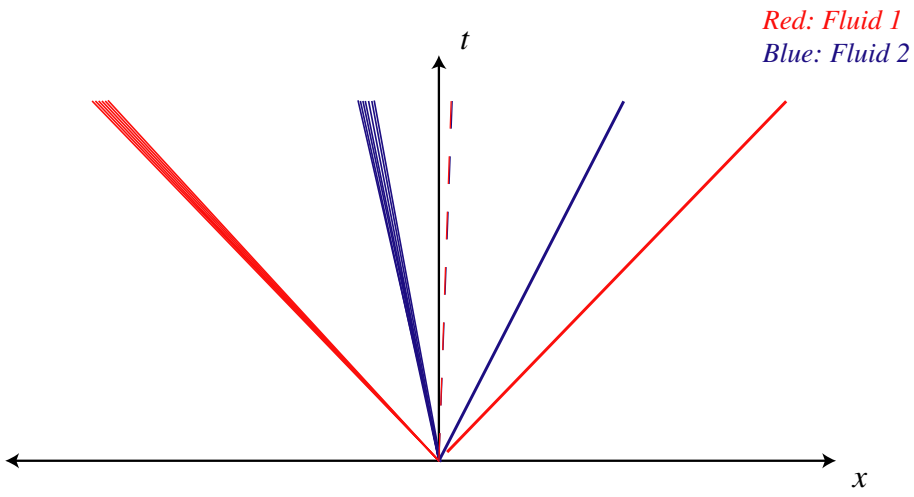

Figure 4: Wave pattern for test 1 with two left rarefactions, 2 right shocks and 3 contact waves

In figures 5 and 6 numerical results are presented. In each one first and second order numerical methods are presented, with the first order method shown on top. For the results shown in figures 5 and 6 we used 100 and 800 cells, respectively. The figures show the density of fluid 1 and the velocity of fluid 2. The exact solution (courtesy of

		ρ_1	u_1	p_1	α_1	ρ_2	u_2	p_2
W_L		0.1×10^4	9.0	0.2×10^7	0.8	0.15×10^1	9.0	0.2×10^6
W_R		0.1×10^4	5.0	0.18×10^6	0.2	0.1×10^1	5.0	0.18×10^6

Table 2: Initial conditions for shock tube problem for liquid and gas

Schwendeman et al.[4]) is shown by the black line. It is observed that results may be improved by going from a first order to a second order scheme or by refining the mesh from 100 to 800 cells. The EVILIN approach is more accurate in the presence of shocks and rarefactions. All three methods produce spurious oscillations near the contact waves, which tend to disappear with mesh refinement. A special comment on slowly moving contacts is in order: these waves are badly smeared by 'non-complete' Riemann solvers, whereas our method recognizes all of them and resolve them properly.

As mentioned above, computational cost can be a limitation when exact Riemann solvers are used. The exact solution presented by Schwendeman et al. is computed iteratively in two steps. In table 3 we compare the computational cost of the exact, EVILIN, StraEv and StraEx Riemann solvers. It is clear that the exact solver is more expensive than the others by a factor of three to five in the first order code. When the order of the method increases this factor reduces to two to three, mainly to the additional reconstruction procedure. An important aspect to emphasize is that as the order of the method increases, the exact Riemann solver pays off. In our computations we observe that the cost increase is about 20 percent for the exact solver, while the others show an increase close to 50 percent.

Method	1^{st} cpu time (s)	ratio	2^{nd} cpu time (s)	ratio
Exact	27.53	1.00	33.68	1.00
EVILIN	8.79	0.32	15.22	0.45
StraEv	7.03	0.25	13.73	0.40
StraEx	5.45	0.19	12.05	0.35

Table 3: Computational cost for numerical methods normalized to the exact Riemann solver for Test 1 with 800 cells and first and second order.

4.2 Test2: Numerical convergence

With this test the numerical convergence rate is tested where the initial condition generates a smooth solution with no discontinuities. In order to have a reference solution, because no exact solution exists, a numerical solution with very fine mesh is used. The initial data was taken from Schwendeman et al.[4] and consists of constant density and pressure for both fluids, constant velocity for fluid 2 and smooth transition for void fraction and for the velocity of fluid 1, as follows.

$$\rho_1(x,0) = \rho_2(x,0) = 1.0, \quad p_1(x,0) = p_2(x,0) = 1.0, \quad v_2(x,0) = 0.0, \tag{24}$$

$$v_1(x,0) = \frac{1}{2} + \frac{1}{2}tanh(20x - 10), \quad \alpha_1(x,0) = \frac{1}{2} + \frac{2}{5}tanh(20x - 8) \tag{25}$$

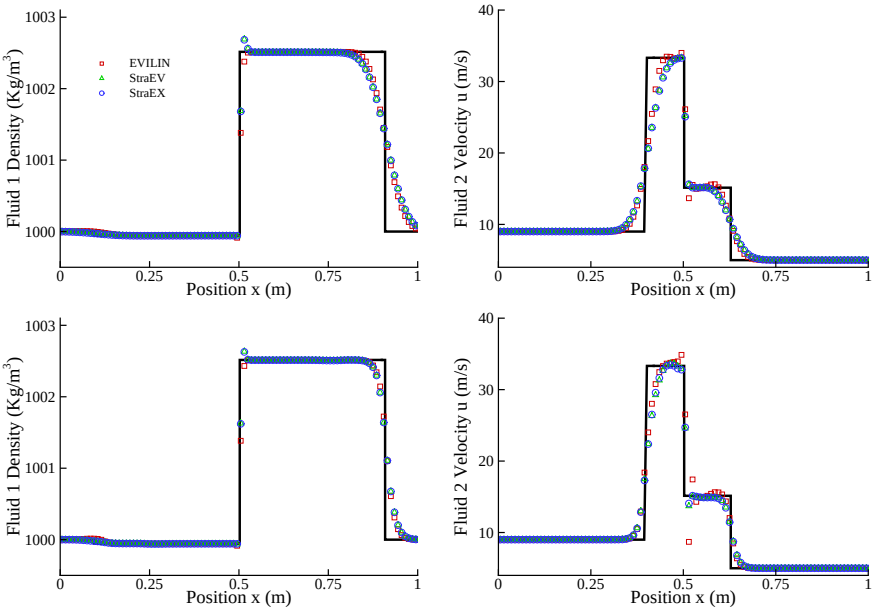

Figure 5: Numerical results for Test 1: First order method on top while second order solution is bellow. 100 cell are used.

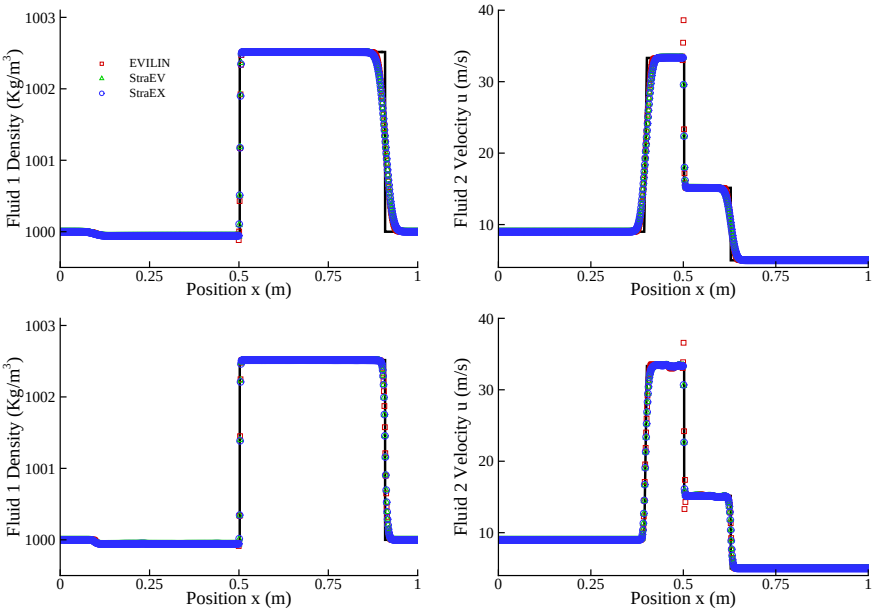

Figure 6: Numerical results for Test 1: First order method on top while second order solution is bellow. 800 cell are used.

Parameters for the equation of state are $\gamma_1 = 4.4$, $p_1^o = 0.0$, $\gamma_2 = 1.4$ and $p_2^o = 0.0$. The computational domain is $[0, 1]$ for times $t \in [0, 0.1]$. Transmissive boundary conditions

are used and four mesh sizes are employed: 100, 200, 400 and 800 cells. The convergence rate and errors are computed using L_1, L_2 and L_∞ norms. Convergence rates for first

Cells	L_1 Error	r	L_2 Error	r	L_∞ Error	r
100	2.24×10^{-4}	0.00	3.82×10^{-4}	0.00	1.48×10^{-3}	0.00
200	5.61×10^{-5}	1.99	9.58×10^{-5}	2.00	3.72×10^{-4}	2.00
400	1.41×10^{-5}	2.00	2.40×10^{-5}	2.00	9.28×10^{-5}	2.00
800	3.52×10^{-6}	2.00	5.99×10^{-6}	2.00	2.31×10^{-5}	2.01

Table 4: L_1, L_2 and L_{inf} norm for EVILIN method with MUSCL_Hancock reconstruction.

Cells	L_1 Error	r	L_2 Error	r	L_∞ Error	r
100	2.25×10^{-4}	0.00	3.84×10^{-4}	0.00	1.44×10^{-3}	0.00
200	5.58×10^{-5}	2.01	9.51×10^{-5}	2.01	3.59×10^{-4}	2.01
400	1.39×10^{-5}	2.01	2.36×10^{-5}	2.01	8.94×10^{-5}	2.01
800	3.46×10^{-6}	2.01	5.88×10^{-6}	2.01	2.22×10^{-5}	2.01

Table 5: L_1, L_2 and L_{inf} norm for StraEv method with MUSCL_Hancock reconstruction.

Cells	L_1 Error	r	L_2 Error	r	L_∞ Error	r
100	2.28×10^{-4}	0.00	3.88×10^{-4}	0.00	1.44×10^{-3}	0.00
200	5.73×10^{-5}	1.99	9.74×10^{-5}	2.00	3.62×10^{-4}	1.99
400	1.43×10^{-5}	2.00	2.44×10^{-5}	2.00	9.05×10^{-5}	2.00
800	3.58×10^{-6}	2.00	6.08×10^{-6}	2.00	2.26×10^{-5}	2.00

Table 6: L_1, L_2 and L_{inf} norm for StraEx method with MUSCL_Hancock reconstruction.

the order scheme are not shown here but the expected order is reached. For second order schemes using TVD limiters the order of convergence is around 1, as expected. If no limiter is used and MUSCL reconstruction is performed, the order 2 is reached in all norms and for all three numerical schemes, see table 4, 5 and 6.

5 CONCLUSIONS

We have presented three alternatives for the solution of the Riemann problem for the Baer-Nunziato multiphase system. The EVILIN approach solves the full seven-equation system, while StraEv and StraEx use the stratification hypothesis to solve smaller and simpler problems. All three approaches constitute complete Riemann solvers. Convergence to second order is reached using MUSCL reconstruction. The computational cost indicates that these three solvers are less expensive than the exact solver and thus represent a promising alternative.

REFERENCES

[1] M. Baer and J. Nunziato. A two-phase mixture theory for the deflagration to detonation transition (DDT) in reactive granular materials. *Int. J. Num. Meth. Engng.*, **12**, 861–889, (1986).

[2] C. Chang and M. Liou. A new approach to the simulation of compressible multifluid flows with AUSM+ scheme. *16th AIAA Computational Fluid Dynamics, Conference.*, (2003).

[3] E.F. Toro. Riemann solvers with evolved initial conditions. *Int. J. Numer. Meth. Fluids. (accepted)*, **00**, 000–000, (2006).

[4] D. W. Schwendeman, C. W. Wahle and A. K. Kapila . The Riemann problem and high-resolution Godunov method for a model of compressible two-phase flow. *Journal of Computational Physics.*, **212**, 490–526, (2006).

[5] R. Saurel and R. Abgrall. A multiphase Godunov method for compressible multifluid and multiphase flows. *Journal of Computational Physics.*, **150**, 425–467, (1999).

[6] C.E. Castro and E.F. Toro. A Riemann solver and upwind methods for a two-phase flow model in non-conservative form. *Int. J. Numer. Meth. Fluids.*, **50**, 275–307, (2006).

[7] N. Andrianov and G. Warnecke. Toro. The Riemann problem for the Baer Nunziato two-phase flow model. *Journal of Computational Physics.*, **195**, 434–464, (2004).

[8] E. Romenski and E. F. Toro. Compressible two-phase flows: Two-pressure models and numerical methods. *Computational Fluid Dynamics Journal*, **13**, 403–416, (2004).

[9] B. H. Stewart and B. Wendroff. Two-phase flow: models and methods. *Journal of Computational Physics*, **56**, 363–409, (1984).

[10] D. Drew. Mathematical Modeling of Two-Phase Flow. *Ann. Rev. Fluid Mech.*, **15**, 261–291, (1983).

[11] M. Ishii. *Thermo-fluid Dynamic Theory of Two-phase Flow*, Eyrolles, Paris, (1975).

[12] D.Gidaspow. *Multiphase Flow and Fluidization: Continuum and Kinetic Theory Descriptions*, Academic Press, (1994).

[13] R. Abgrall. How to prevent pressure oscillations in multicomponent flow calculations: A quasi conservative approach. *Journal of Computational Physics*, **125**, 150–160 , (1996).

[14] M. J. Ivings, D. M. Causon and E. F. Toro. On Riemann Solvers for Compressible Liquids. *Int. J. Numer. Meth. Fluids.*, **28**, 395–418 , (1998).

[15] P. Embid and M. Baer. Mathematical analysis of a two-phase continuum mixture theory. *Continuum Mechanics and Thermodynamics.*, **4**, 279–312 , (1992).

[16] C. Chang and M. Liou. A conservative compressible multifluid model for multiphase flow: Shock-inteface interaction problems. *17th AIAA Computational Fluid Dynamics, Conference.*, (2005).

[17] B van Leer. On the Relation Between the Upwind-Differencing Schemes of Godunov, Enguist-Osher and Roe. *SIAM J. Sci. Stat. Comput.*, **5**, 1–20 , (1985).

[18] E. F. Toro. *Riemann solvers and numerical methods for fluid dynamics. Second Edition*, Springer, Berlin Heidelberg, (1999).

[19] E. F. Toro. Multi-Stage Predictor-Corrector Fluxes for Hyperbolic Equations. *Isaac Newton Institute for Mathematical Sciences Preprint Series NI03037-NPA*. University of Cambridge. UK